Eur. Phys. J. D **9**, 561–564 (1999)

THE EUROPEAN PHYSICAL JOURNAL D

EDP Sciences

Simulation of the submonolayer homoepitaxial clusters growth on Ag(110)

C. Mottet, R. Ferrando[a], F. Hontinfinde[b], and A.C. Levi

INFM and CFSBT/CNR, Dipartimento di Fisica dell'Università di Genova, via Dodecaneso 33, I-16146 Genova, Italy

Received: 1 September 1998 / Received in final form: 16 October 1998

Abstract. The submonolayer growth of Ag/Ag(110) is studied by kinetic Monte Carlo simulations including deposition, diffusion, and fully reversible aggregation with both anisotropic diffusion barriers and anisotropic bond energies. The barriers for the elementary diffusion processes, including the Schwoebel barrier at step borders, are calculated by many-body tight-binding potentials. Depending on growth conditions (temperature T, adatom flux F, and coverage θ) the model shows morphology transitions to one-dimensional (1D) in-channel strips and then to 2D or 3D compact islands. At low T, the island density n_{I} versus θ shows the nucleation, growth (at saturation density), and the coalescence regimes, whereas at higher T, at which point detachment from islands becomes effective, n_{I} presents a maximum at very low θ, followed by a decrease, at first caused by island dissolution and then, for higher θ, by coalescence.

PACS. 81.15.Aa Theory and models of film growth – 81.15.Hi Molecular, atomic, ion, and chemical beam epitaxy – 82.30.Nr Association, addition, insertion, cluster formation, hydrogen bonding

1 Introduction

Diffusion-controlled aggregation on crystal surfaces during homo- or heteroepitaxy allows the production of a large variety of nonequilibrium nanostructures of both fundamental and technological interests. Such a control of the shape, size, and density of the islands is now performed experimentally (mainly by STM) [1–3] and has stimulated much theoretical work [4–6]. A model with edge diffusion on a rectangular substrate has been proposed for the interpretation of growth data on Cu/Pd(110) [7], but reversible aggregation (i.e., the detachment of atoms from islands) has been included in few models [8], because it is computationally more demanding.

We propose here a kinetic Monte Carlo simulation of a model for the growth of Ag(110), with deposition, diffusion, and fully reversible aggregation on a rectangular substrate with both anisotropic diffusion barriers and anisotropic bond energies. The energy barriers are calculated by quenched molecular dynamics (MD), and Ag is modeled by many-body tight-binding potentials [9, 10]. Results at very low coverage θ ($\theta < 0.05$ ml) have been presented [11, 12]. There it has been shown that at fixed adatom flux F (or at fixed temperature T) and increasing T (or decreasing F), the morphology of the islands changes dramatically from small isotropic clusters at very low T (or very high F) to well-separated one-dimensional (1D) strips along the in-channel $[1\bar{1}0]$ direction, and 2D anisotropic islands at high T (or slow F). Such a result is, qualitatively, in good agreement with the observation by STM of the morphology transition from 1D to 2D islands in the low-θ deposition of Cu on Pd(110) by increasing T [3]. The advantage of the simulation is that one may gain further understanding of the microscopic origin of the morphology transition: First, it has been shown in [11] that the growth of 1D strips and the subsequent morphology transition to 2D islands is possible because of the *anisotropy of bonding* (the *anisotropy of diffusion* playing a minor role); and second, the microscopic mechanism of that transition is *adatom detachment, terrace diffusion and reattachment* (not necessarily to the same island) [12] rather than *corner rounding* from the end of a chain to its edge [7]. The effect of the different anisotropies (diffusion versus sticking) related to Ag and Cu have been investigated, and the results show that faster surface diffusion in Cu gives longer 1D strips than those in Ag at the same θ (0.05 ml), given that sticking is anisotropic [12]. Finally, the behavior of adatom (monomer) and island densities has been presented for $\theta < 0.05$, and shows that in both metals, scaling holds in limited F and T ranges, and the exponents depend on T [12]. In this paper, we extend the study to higher coverages, including the Schwoebel barrier effect that occurs when adatoms fall on preexisting islands, in order to investigate a full 3D model on the submonolayer homoepitaxial growth of Ag(110).

The paper is organized as follows. In Sect. 2, the 3D model is described. In Sect. 3, the results on the morph-

[a] Corresponding author. e-mail: `ferrando@fisica.unige.it`

[b] *Present address*: IMSP, Université Nationale du Benin, BP 613 Porto Novo (Benin)

ology and on the density of islands are presented and discussed. Sect. 4 contains the conclusions.

2 The model

In our simulations, the atoms are deposited randomly on a rectangular substrate with flux F per site. Once the atoms are deposited, they can diffuse, aggregate and dissociate with the frequency r_k for a given process k of barrier E_k, given by the usual Arrhenius expression:

$$r_k = \nu \exp\left(-\frac{E_k}{k_{\mathrm{B}}T}\right), \tag{1}$$

where ν is the prefactor (taken equal to $10^{12}\,\mathrm{s}^{-1}$ [13]) and k_{B} is the Boltzmann constant. When θ increases, the probability of direct impact on preexisting islands is not negligible. In this situation, adatoms can diffuse on the islands and jump (or exchange) down to the lower terrace. The calculation of the energy barriers by the many-body Rosato, Guillopé and Legrand (RGL) potential [9] are detailed elsewhere [10] together with the approximation of the anisotropic bond-breaking model (ABBM) [11,12]. By the ABBM approximation, it is possible to lower significantly the number of processes that are relevant for the diffusion on the (110) surfaces. The ABBM is based on two assumptions:

(1) For a given process k, E_k depends only on the environment of the diffusing adatom in the *initial* position.
(2) E_k can be computed by the addition of contributions from in-channel and cross-channel bonds to the barrier for the diffusion of an isolated adatom.

In this way, the energy barrier for a given process is written as

$$E_p = E_p^{\mathrm{d}} + n_p E_p^{\mathrm{b}} + n_n E_n^{\mathrm{b}} \tag{2}$$

$$E_n = E_n^{\mathrm{d}} + n_p E_p^{\mathrm{b}} + n_n E_n^{\mathrm{b}}; \tag{3}$$

where $E_{p,n}^{\mathrm{d}}$ are the barriers for diffusion of free adatom on the surface ($E_{p,n}^{\mathrm{d}} = E_{p,n}^{0}$ for intralayer diffusion processes, and $E_{p,n}^{\mathrm{d}} = E_{p,n}^{1}$ for interlayer diffusion processes, i.e., step descent); $E_{p,n}^{\mathrm{b}}$ and $n_{p,n}$ are the strengths and numbers of in-channel and cross-channel bonds. We take the values $E_p^0 = 0.28\,\mathrm{eV}$, $E_n^0 = 0.38\,\mathrm{eV}$, $E_p^1 = 0.34\,\mathrm{eV}$, $E_n^1 = 0.56\,\mathrm{eV}$, $E_p^{\mathrm{b}} = 0.18\,\mathrm{eV}$, and $E_n^{\mathrm{b}} = 0.02\,\mathrm{eV}$ for Ag. We notice that the ABBM is very accurate in reproducing the actual barriers on the Ag and Cu(110) surfaces [12], whereas the use of bond-breaking models for metals in general is not correct (for example in the (100) surface). The kinetic Monte Carlo (KMC) simulation is performed by the algorithm developed by Bortz, Kalos, and Lebowitz (BKL) [14]; in this model, a move is executed at each step according to its *a priori* probability. At a given time, in a given configuration C, the surface is characterized by all the site rates $r_i(C)$. $r_i(C)$ is the sum of five partial rates $p_i^j(C)$ corresponding to deposition and diffusion in the four directions on the surface. We neglect cross-channel diffusion in diagonal directions. In fact, we have checked [12] that diagonal exchange diffusion has no significant effect on the growth. The $r_i(C)$ are at the bottom of a binary tree which the algorithm builds by making the two-by-two sums of the site rates to get the total rate $R(C)$. The dimensions of the tree obey the relation $N = 2^L$, where N is the number of nodes at the bottom of the tree (greater or equal to the total number of sites in the lattice), and L is the number of levels of the tree. The algorithm chooses a site i randomly by going down the binary tree from the total rate $R(C)$ to the site rate $r_i(C)$, choosing randomly at each level l one of the two branches of the tree. Then a random number r ($0 < r < r_i(C)$) is extracted, and the process j, which satisfies $p_i^{j-1}(C) < r < p_i^j(C)$, is selected and executed. All modified rates are reactualized to take into account the local change of the surface configuration after the move. In this way, simulations keep reasonable computer time when the number of adatoms increases. The size of the simulated surface is typically of 200×200 sites with periodic boundary conditions. Averages are taken over 10 to 20 runs.

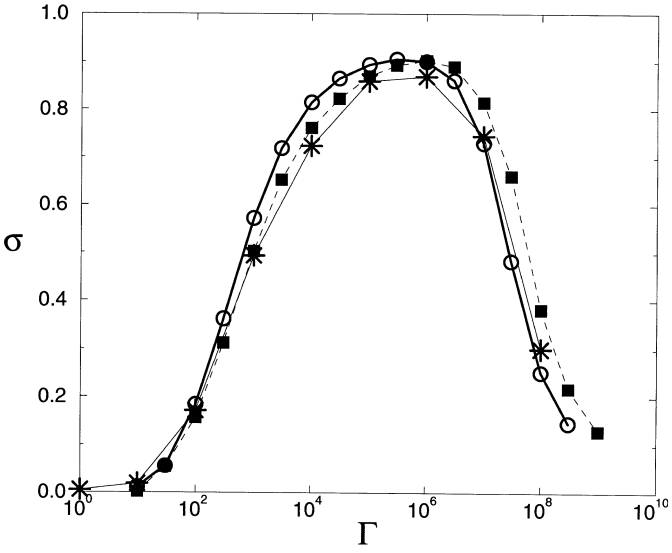

Fig. 1. Bond anisotropy parameter σ as a function of $\Gamma = D_p/F$ at $T = 250$ K and $\theta = 0.05$ ml for the 2D (squares) and 3D (stars) models.

3 Results

In order to check the assumption that the deposition of adatoms above preexisting islands can be neglected at low θ, we perform simulations with the full 3D model described above, but at low θ ($\theta = 0.05$ ml), and we compare the results with other calculations performed at the same θ without deposition on islands [12]. As our 3D model does not include diagonal cross-channel diffusion, we have made the same assumption in the 2D model (where deposition above islands is not allowed). In Fig. 1, we plot the direc-

tional bond-counting parameter σ, [11, 12] defined as

$$\sigma = \frac{\overline{n}_p - \overline{n}_n}{\overline{n}_p + \overline{n}_n}, \tag{4}$$

where $\overline{n}_p$ and $\overline{n}_n$ are the average number of in-channel and cross-channel neighbor bonds, respectively, as a function of $\Gamma = D_p/F$, where D_p is the hopping rate of an isolated adatom in the in-channel direction:

$$D_p = \nu \exp\left(-\frac{E_p^0}{k_\mathrm{B}T}\right). \tag{5}$$

The case $T = 250$ K, $\theta = 0.05$ ml is considered. In Fig. 1, the squares and the stars refer to the 2D and 3D models, respectively. The overall aspect of the curve has already been discussed in detail elsewhere [11, 12]. Let us recall that at low Γ (i.e., high F), small isotropic clusters are formed; then, at intermediate Γ, $\sigma \simeq 1$ and well-defined 1D in-channel strips are present; and finally, at high Γ (i.e., low F), large 2D anisotropic islands are obtained. The results in Fig. 1 show that there is no significant difference between the 2D and 3D model up to $\theta = 0.05$; below this coverage, direct impacts onto preexististing islands have, in practice, no effects on the morphologies. In the following, we consider the full 3D model in order to investigate the growth of one monolayer of Ag on a Ag(110) substrate starting from a flat surface and at a constant flux ($F = 1$ ml/min). In Fig. 2, the morphological parameter σ is presented as a function of θ, at three different temperatures. At low T (140 K), σ keeps low values during the growth, with a maximum of about 0.4 for $\theta = 0.1$, and a decrease to $\sigma = 0.2$ for $\theta = 1$. At high T (240 K), σ starts from 1, showing that 1D linear chains are formed at very low θ ($\theta < 0.01$ ml), and then it decreases to a value near zero at the completion of the monolayer. At an intermediate T ($T = 200$ K), σ keeps a value near 1 up to $\theta \sim 0.1$; this means that 1D strips can be obtained on a quite large range of coverages. After that, σ decreases to a value of 0.2, as in the low T case. The morphology of the islands is illustrated in Fig. 3 by snapshots taken at $\theta = 0.25$ and $\theta = 1$ and for the three different temperatures. It can be seen that at low T, nearly isotropic 3D islands are obtained, and the surface is rough at the monolayer completion. At $T = 200$ K, the islands are anisotropic and quite 2D, but the surface obtained after the deposition of one monolayer presents some double steps, meaning that we have not reached a layer-by-layer growth regime. At 240 K, such a regime is reached. Finally, we present in Fig. 4 the island density n_I and the adatom (monomer) density n_A as functions of θ, up to one monolayer at the three different T. In the low T case, we recover a dynamical behavior comparable to the one obtained in a submonolayer molecular-beam epitaxy model for the dendritic island growth [6]. In that model (on a square lattice), the diffusion of adatoms is limited by lateral aggregation to preexisting islands or to other adatoms, and the dependences of n_I and n_A versus θ are interpreted as following different regimes. In the first stage of the growth, there is a nucleation regime; there, n_I is much smaller than n_A, so that the probability of island growth is much smaller than the probability

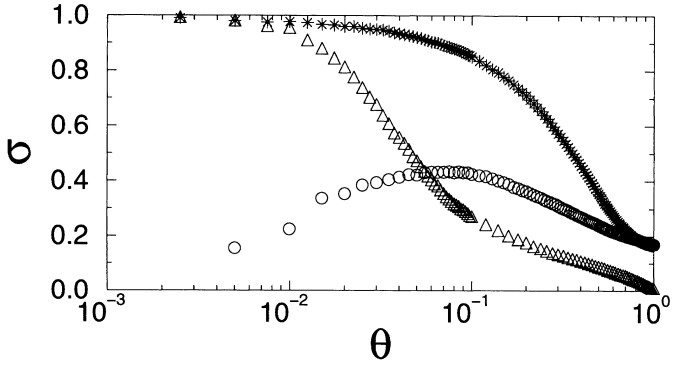

Fig. 2. Bond anisotropy parameter σ as a function of θ at constant $F = 1$ ml/min and for different temperatures $T = 140$ K (circles), $T = 200$ K (stars), and $T = 240$ K (triangles).

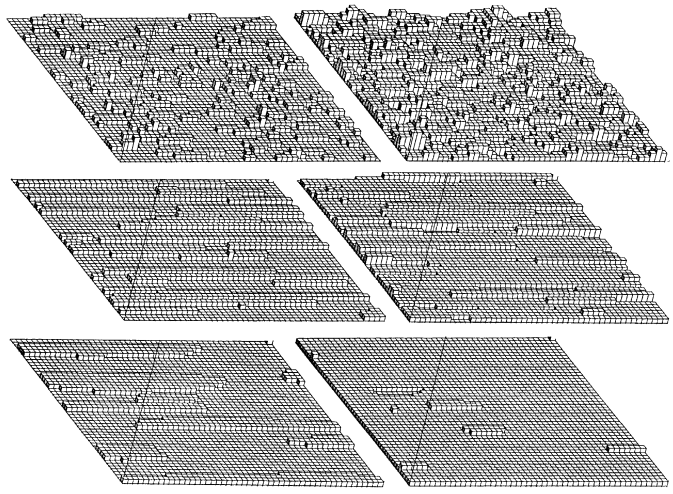

Fig. 3. Morphologies of the surface for a 50×50 section of a 200×200 simulation box at fixed flux $F = 1$ ml/min and various coverages and temperatures: left column, $\theta = 0.25$ ml; right column, $\theta = 1$ ml; top line, $T = 140$ K; middle line, $T = 200$ K; and bottom line, $T = 240$ K.

of nucleation. As θ increases, n_A reaches a maximum and then begins to decrease, whereas n_I tends to saturate. This regime is called the aggregation regime: The adatom density decreases even if deposition goes on. Adatoms can reach easily the edges of the islands present on the surface, but the probability for their meeting another free adatom is now small, so n_I saturates, and the size of the islands increases. At larger θ, the islands become so large that they coalesce. It is in the last regime that n_I drops suddenly. At intermediate T, n_I behaves as at low T, but the maximum in n_A is already reached at extremely low coverage, and it is not seen in the Fig. 4. At high T (240 K), the behavior of our model cannot be interpreted at all as at 140 K. In fact, the maximum of n_I is reached at very low θ (nearly one order of magnitude smaller than at 140 K), well before the coalescence regime. In this case, the decrease of n_I is due to the morphology transition from 1D linear strips to 2D anisotropic islands (see the triangles in Fig. 2 and notice that the drop of σ happens in the same θ range in which

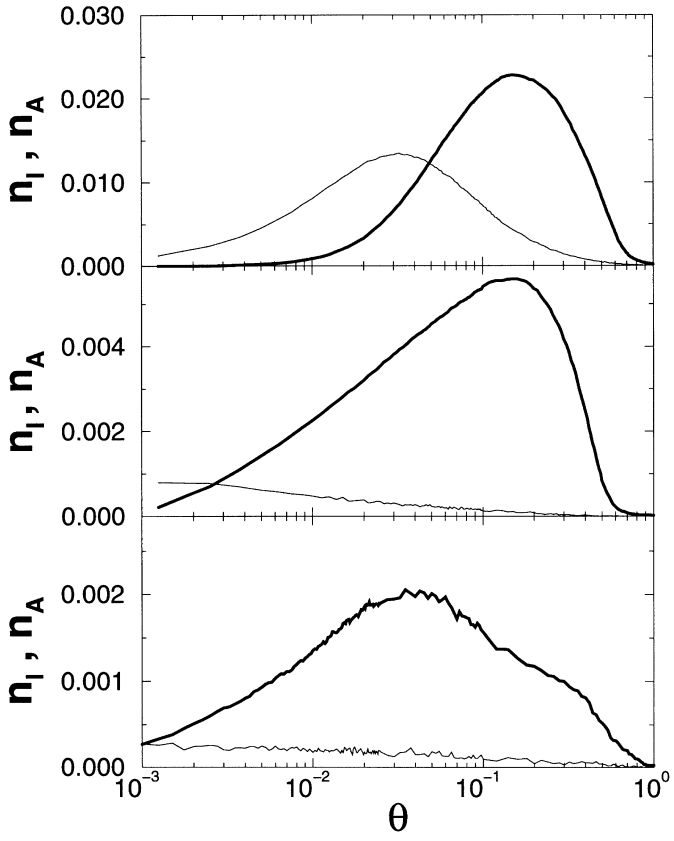

Fig. 4. Island density n_{I} (thick line) and adatom density n_{A} (thin line) as functions of coverage θ at fixed flux $F = 1$ ml/min and different temperatures: $T = 140$ K, $T = 200$ K, $T = 240$ K from top to bottom.

n_{I} starts to decrease). Such transition involves linear chain dissolution via adatom detachment from the end of the strips and reaggregation on other more compact islands. The onset of ripening during growth has already been obtained by Ratsch *et al.* [8], in an isotropic model with atom detachment from island edges. Only at much higher θ does coalescence become effective in reducing the island density.

4 Conclusions

We have presented a kinetic Monte Carlo simulation of the Ag(110) 3D homoepitaxial growth of one monolayer on a flat substrate. The model includes deposition, surface diffusion (with both inter- and intralayer movings) and fully reversible aggregation. The energy barriers for the elementary diffusion processes are determined by the molecular dynamics technique with the many-body RGL potential. At a given flux, we have analyzed the behavior of our model at different temperatures in the full coverage range from 0 to 1 monolayers. The character of the growth changes from three-dimensional to layer-by-layer when T is increased. Depending on the temperature and on the coverage, 1D, 2D, and 3D islands are obtained. At high temperature and low coverage, well before the onset of coalescence, the island density drops suddenly and the morphology transition from 1D to 2D aggregates takes place. The transition is due to adatom detachment from the ends of the chains. These results show clearly the onset of island dissolution and ripening during growth.

References

1. Y.W. Mo, J. Kleiner, M.B. Webb, M. Lagally: Phys. Rev. Lett. **66**, 1998 (1991)
2. J.A. Stroscio, D.T. Pierce: Phys. Rev. B **49**, 8522 (1994)
3. H. Röder, E. Hahn, H. Brune, J.P. Bucher, K. Kern: Nature **366**, 141 (1993); E. Hahn, E. Kampshoff, A. Fricke, J.P. Bucher, K. Kern: Surf. Sci. **319**, 277 (1994)
4. J. Villain, A. Pimpinelli, L. Tang, D. Wolf: J. Phys. (Paris) I **2**, 2107 (1992)
5. A.-L. Barabási, H.E. Stanley: *Fractal Concepts in Surface Growth* (Cambridge University Press 1995)
6. J.G. Amar, F. Family, P.M. Lam: Phys. Rev. B **50**, 8781 (1994)
7. Y. Li, M.C. Bartelt, J.W. Evans, N. Waelchli, E. Kampshoff, K. Kern: Phys. Rev. B **56**, 12 539 (1997)
8. C. Ratsch, A. Zangwill, P. Šmilauer, D.D. Vvedensky: Phys. Rev. Lett. **72**, 3194 (1994)
9. V. Rosato, M. Guillopé, B. Legrand: Philos. Mag. A **59**, 321 (1989)
10. F. Hontinfinde, R. Ferrando, A.C. Levi: Surf. Sci. **366**, 306 (1996)
11. R. Ferrando, F. Hontinfinde, A.C. Levi: Phys. Rev. B **56**, 4406 (1997)
12. C. Mottet, R. Ferrando, F. Hontinfinde, A.C. Levi: Surf. Sci. **417**, 220 (1998)
13. R. Ferrando: Phys. Rev. Lett. **76**, 4195 (1996)
14. A.B. Bortz, M.H. Kalos, J.L. Lebowitz: J. Comp. Phys. **17**, 10 (1975); P.A. Maksym: Semicond. Sci. Technol. **3**, 594 (1988); M. Kotrla: Comp. Phys. Commun. **96**, 82 (1996)